Am J Transl Res 2019;11(6):3779-3789
www.ajtr.org /ISSN:1943-8141/AJTR0091305

Original Article

Establishment of the PDTX model of gynecological tumors

Wen Yang[1*], Wen-Sheng Fan[1*], Ming-Xia Ye[1*], Zhen Li[1], Cheng-Lei Gu[1], Yan-Ping Zhu[2], Yan-Peng Hao[2], Zhi-Qiang Wang[2], Li Wang[2], Yuan-Guang Meng[1]

[1]Department of Obstetrics and Gynecology, Chinese PLA General Hospital, 28 Fuxing Road, Haidian District, Beijing 100853, China; [2]Nanjing Personal Oncology Biological Technology Co. Ltd., 568 Longmian Road, Jiangning District, Nanjing 211100, Jiangsu, China. [*]Equal contributors.

Received January 14, 2019; Accepted May 25, 2019; Epub June 15, 2019; Published June 30, 2019

Abstract: Objective: Fresh tumor tissues from patients with gynecological tumors were obtained by surgery or biopsy, and transplanted into NOD-Prkdcem26Il2rgem26Nju (NCG) mice to establish a patient-derived tumor xenograft (PDTX). Materials and methods: A total of 15 patients with gynecologic tumors were enrolled into the present study. Among these patients, 12 patients had epithelial fallopian tube/ovarian/peritoneal cancer, one patient had metastatic ovarian cancer, and two patients had cervical cancer. Furthermore, among these patients, three patients were treated with puncture or microscopy biopsy, six patients underwent laparoscopic surgery, and six patients underwent robotic surgery. The tumor formation latency, tumor formation rate, tumor volume, tumor invasion and metastasis of the transplanted tumor were observed, the consistency of the PDTX model tumor tissue and patient's primary tumor tissue was compared by pathological H&E staining, and pharmacodynamics testing was performed. Results: Seven of 15 PDTX models were successfully established, with a success rate of 46.7%. The tumor formation time ranged within 21-130 days, with a median tumor formation time of 73 days. The PDTX model maintained the differentiation, morphological and structural characteristics of tumor cells, and the pharmacodynamic test was completed in five patients. Conclusion: The PDTX model is highly consistent with the pathology of the patient's tumor, and can be used as a substitute for clinical patients to guide the accurate treatment and scientific research of gynecological tumors.

Keywords: Gynecological tumors, PDTX, xenograft model, pharmacodynamic screening

Introduction

Tumors have become one of the most serious diseases that threaten human life in modern society. In gynecological tumors, ovarian cancer, cervical cancer and endometrial cancer remain as the most important female reproductive tract malignancies that threaten women's health. Chemotherapy with cytotoxic drugs is an important treatment for advanced gynecologic tumors. However, the efficacy of most anti-tumor chemotherapy drugs remains unsatisfactory. Furthermore, the objective effective rate of chemotherapy in clinical practice differs. Therefore, there is an urgent need to determine how to select the appropriate chemotherapy drug and/or regimen for a certain patient to improve the efficacy of chemotherapy in clinical practice. At present, the main methods for tumor pharmacodynamic testing are *in vitro* drug evaluation using human tumor cell lines and the *in vivo* pharmacodynamic testing of xenograft models. However, since the established standard tumor cell line irreversibly loses important biological properties of the original tumor (such as tumor stromal cells, vascular components, cytokines, etc.), it does not fully reflect the phenotype or genomic feature type of the original tumor [1-3]. The patient-derived tumor xenograft (PDTX) model establishes an animal xenograft model in severely immunodeficient mice (SCID) with fresh tumor tissues surgically resected or biopsied, and the PDTX model retains the tumor tissue. Heterogeneity, which retains human stromal cells, vascular tissues and cytokines, maintains the microenvironment of the tumor tissue, and is an ideal model for clinical research and phar-

macodynamic tests. PDTX models, such as breast cancer, lung cancer, pancreatic cancer, brain tumor and colon cancer, have been widely used in preclinical drug detection and biomarker identification [4]. Recently, there have been reports of the establishment of a PDTX model for gynecologic oncology. However, the methods of vaccination are different [5-10]. In the present study, the PDTX model was established using tumor tissues obtained by clinical operation or biopsy. Histopathology and pharmacodynamic tests were carried out to further explore the feasibility of establishing a stable preclinical drug screening platform.

Materials and methods

Experimental animals

A total of 262 SPF-grade female NCG mice, which were 6-8 weeks old and weighed 20 ± 2 g, were purchased from the Nanjing University Model Animals Institute. These animals were housed in an SPF-grade animal facility at 25 ± 2°C with a humidity of 40%-70%. In addition, 12-hour/12-hour was alternated between day and night, and these mice were given a free diet. Before the experiment, these mice were adaptively reared for more than three days.

Reagents and consumables

The following were used: Leibobitz's L15 tissue preservation solution (containing L-glutamine), 10% neutral formaldehyde, penicillin and streptomycin (pen/strep), disposable surgical equipment, gauze, etc.

Tumor specimen source and treatment

Fresh tumor tissues were collected from 15 patients by surgery or biopsy in the Department of Obstetrics and Gynecology of the General Hospital of the PLA (**Table 1**). After the operation or biopsy, the specimens were immediately placed in the tissue preservation solution and transported to the laboratory. Then, the necrotic substance on the tissue surface was removed, and blood was cleaned on an ultraclean workbench. Afterwards, the tumor transplantation was conducted within 12 hours after sampling.

Tumor transplantation method and passage

The better viable part was selected from freshly obtained tumor tissues, and was cut into small pieces of approximately 2.0 × 2.0 × 2.0 mm^3 with tissue scissors in a medium containing 1% pen/strep. The side skin from the forelimbs was disinfected with alcohol, a trocar was inserted into the skin under the back, and the tumor tissue was quickly injected into the skin. Then, the needle was rotated and pulled out. Blood was removed with an alcohol swab to prevent residual blood from causing biting in mice. Each case based on the size of the specimen was transplanted into 3-8 mice. The animals were weighed twice a week. When the tumor formed, the long diameter and broad diameter of the tumor were measured twice a week, and the relative tumor volume (relative tumor volume = 0.5 × long diameter × short $diameter^2$) was calculated. P2 passage was performed when the P1 generation tumor reached 500 mm^3.

Model monitoring indicator

The general condition of mice was observed daily (including hair color, mental state, activity, diet, etc.). Furthermore, the growth of local subcutaneously transplanted tumors was observed and recorded. When the transplanted tumor tissue reached the size of soybean micro-nodules (≈ 60 mm^3), this was regarded as the tumor formation latency. Then, the tumor formation rate, survival rate and mortality of the mice were observed and recorded. After mice were sacrificed, the transplanted tumors were taken out, and the appearance of the transplanted tumors was observed. The tumor specimens of each patient and transplanted tumor were subjected to routine pathological section and hematoxylin-eosin (H&E) staining to observe the histomorphological features of the tumors.

Pharmacodynamic test

When the passaged tumors reached 100-150 mm^3, these were randomly divided into groups and treated with different regimens. The tumor volume of mice was measured twice a week. After the samples were collected, these were photographed, and the tumor inhibition rate of each group was calculated. Tumor inhibition rate = (control group tumor volume - experimental group tumor volume)/control tumor volume × 100%.

Statistical methods

The software program SPSS 20.0 was used to conduct the statistical analysis. Continuous

Table 1. General situation of the PDTX modeling

Serial No.	Patient No.	Age (year)	Diagnosis	Pathological type	Pathological grading	Stage	Sampling method	Modeling situation	Tumor formation time (day)
1	130112	73	Cervical cancer	Squamous cell carcinoma	G2	IB1	Biopsy	Positive*	80
2	110158	52	Cervical cancer	Squamous cell carcinoma	G2	IB2	Biopsy	Positive*	21
3	110102	34	Ovarian metastatic carcinoma (digestive tract tumor)	Signet ring cell carcinoma	G3	IV	Robot	Negative	
4	110103	57	Ovarian cancer	Adenocarcinoma	G3	IIIC	Laparoscope	Negative	
5	110113	50	Ovarian cancer	Endometrioid carcinoma	G1	IA	Robot	Negative	
6	A11035	51	Ovarian cancer	Clear cell carcinoma	G3	N/A	Laparoscope	Negative	
7	A10043	68	Fallopian tube carcinoma	Serous adenocarcinoma	G3	IA	Robot	Negative	
8	130140	55	Fallopian tube carcinoma	Serous adenocarcinoma	G1	IIB	Puncture	Positive*	73
9	130141	61	Ovarian cancer	Serous adenocarcinoma	G3	IIIC	Robot	Negative	
10	110164	60	Peritoneal cancer	Serous adenocarcinoma	G2	IIIC	Laparoscope	Positive*	89
11	110179	60	Peritoneal cancer	Serous adenocarcinoma	G2	IIIC	Robot	Negative	
12	0101001	53	Recurrent ovarian cancer	Adenocarcinoma	G3	IIIC	Laparoscope	Positive	130
13	0101005	43	Recurrent ovarian cancer	Serous adenocarcinoma	G3	IIB	Laparoscope	Positive	68
14	0101007	58	Ovarian cancer	Serous adenocarcinoma	G3	IIIC	Robot	Positive*	28
15	0101012	47	Ovarian cancer	Serous adenocarcinoma	G3	IIIB	Laparoscope	Negative	

*PDTX model was successfully established.

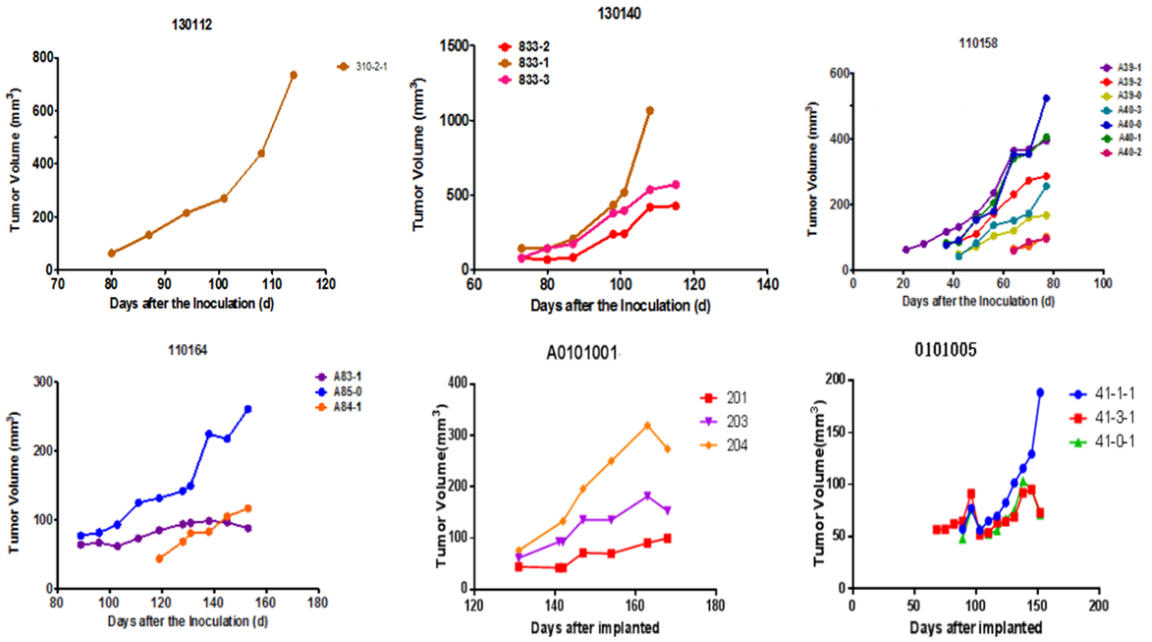

Figure 1. Tumor volume/time growth curve of P1 generation of mice after transplantation: From 21 to 130 days after tumor tissue transplantation, a solid mass with a slightly hard texture that protruded from the skin was observed. Seven of the 15 PDTX models were successful, with a success rate of 46.7%. The tumor formation time ranged from 21 days to 130 days, with a median formation time of 73 days. There was no natural regression after the tumor exceeded 100 mm^3.

variables were expressed as mean ± standard deviation (SD), while non-continuous variables were expressed in percentage.

Results

Mice growth

On the 2nd day after inoculation, the mental state of mice recovered well, the activity was better, and the diet and hair color were normal.

The growth latency of mice tumors and growth of tumor-bearing mice

From 21 to 130 days after tumor tissue transplantation, a solid mass with a slightly hard texture that protruded from the skin was observed. The growth curve of each sample is presented in **Figure 1**. As the tumors continued to increase, some mice had different degrees of weight loss, arched back, and so on. When the tumor volume was ≥ 500 mm^3 (**Figure 2**), passage was carried out. At approximately four weeks after passage, the tumor volume of the P2 generation exceeded 60 mm^3, and the grouping was conducted at approximately six weeks after passage to carry out the pharmacodynamic test.

Mouse tumor formation rate and tumor growth rate

Seven of the 15 PDTX models were successful, with a success rate of 46.7%. Furthermore, the tumor formation time ranged from 21 days to 130 days, with a median formation time of 73 days. There was no natural regression after the tumor exceeded 100 mm^3 (**Figure 1**).

Histopathological examination of patient specimens and transplanted tumors

When tumors in these tumor-bearing mice grew large enough, or when there was obvious weight loss and hair loss, mice were euthanized, and the transplanted tumors were collected. The surface of the tumors was smooth, showing a round or round-like solid tumor, and the texture was slightly hard (**Figure 2**).

Histopathological test

The patient specimen and transplanted tumor specimen were made into pathological sec-

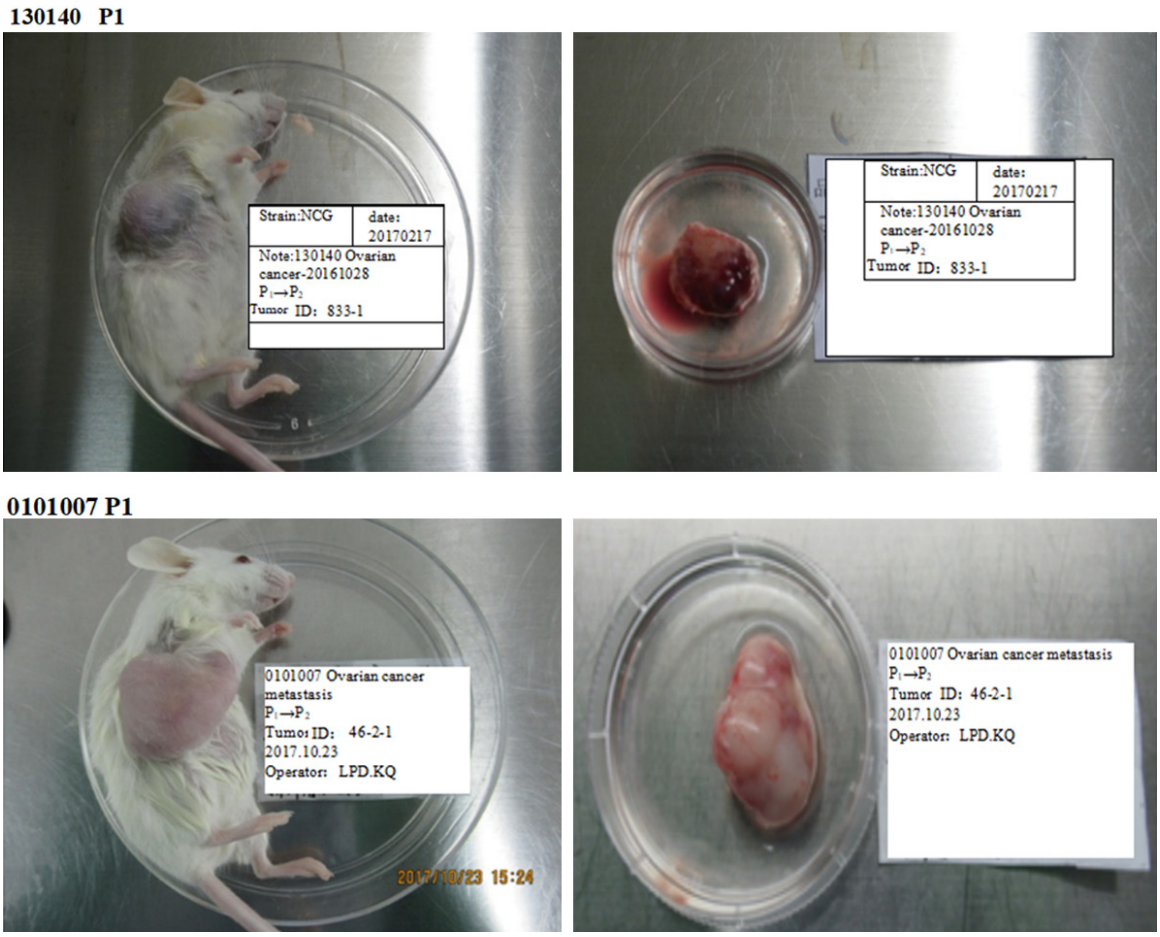

Figure 2. Mouse tumor-bearing condition: As the tumors continued to increase, some mice had different degrees of weight loss and arched back. When the tumor volume was ≥ 500 mm^3, passage was carried out. The surface of the tumors was smooth, showing a round or round-like solid tumor, and the texture was slightly hard.

tions, and subjected to H&E staining, followed by observation under a 400-fold light microscope. The consistency of the tumor pathology from PDTX mice (130112, 130140, 110158, 110164 and 0101007) was compared with that from the original patients (**Figure 3**).

Pharmacodynamic test results

Pharmacodynamic tests were performed on five of seven successful models, which involved 24 different therapeutic regimens. The therapeutic effect of each scheme varied in the PDTX models (**Figures 4** and **5**). For specimen 130112, the combination of cisplatin, doxorubicin and cyclophosphamide had the best effect, with a tumor inhibition rate of 57.5%. For specimen 130140, cisplatin, carboplatin, and the combination of paclitaxel and lobaplatin had a significant effect, with a tumor inhibition rate of 95.7%, 92.4% and 92.8%, respectively. For specimen 110164, the combination of bevacizumab, paclitaxel and cisplatin had the best effect, with a tumor inhibition rate of 71%. For specimen 110158, the combination of bevacizumab and cisplatin exhibited the best effect, with a tumor inhibition rate of 67.1%. For specimen 0101007, both cyclophosphamide and doxorubicin liposomes were effective, with a tumor inhibition rate of 65.71% and 63.09%, respectively.

Discussion

The PDTX model maintains the differentiation, morphological, structural and molecular characteristics of tumor cells. To some extent, the blood supply characteristics, matrix characteristics, growth and necrosis of transplanted tumors in mice are consistent with those of human tumors, providing an important and highly consistent *in vivo* model for drug therapy for tumors. For example, Pierre EC *et al.* transplanted fresh tumor tissues from 77 patients

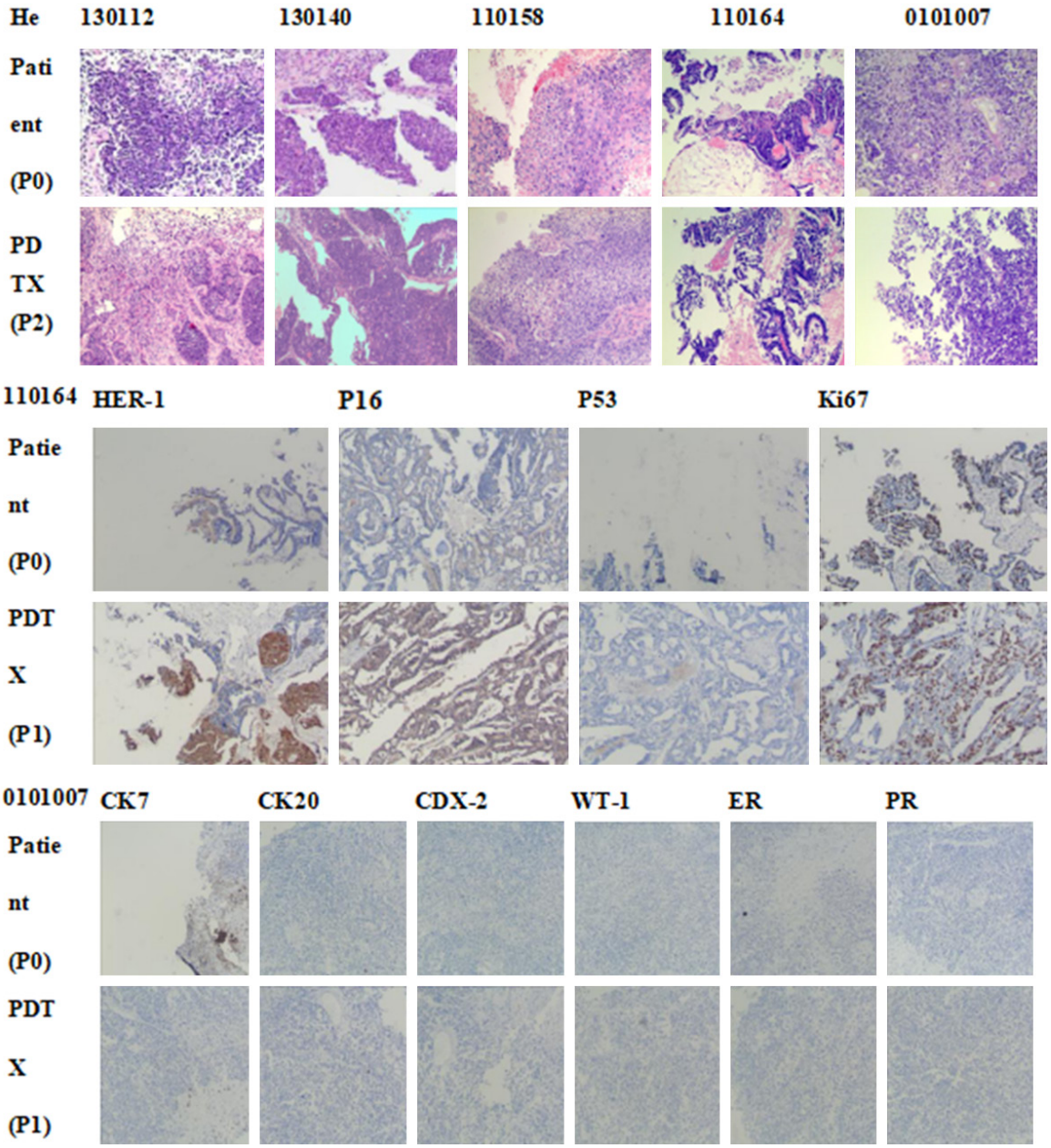

Figure 3. The comparison of pathological consistency between the primary tumor of patients and the PDTX model mice tumor. The results are basically consistent. The patient specimen and transplanted tumor specimen were prepared into pathological sections and subjected to H&E staining, followed by observation under a 400-fold light microscope.

with ovarian cancer into nude mice to establish PDTX models, among which 35 were successful [11]. These results revealed that the histomorphological features of the primary tumor tissues of patients with tumor and ovarian cancer in the PDTX model were basically the same, and the gene expression profiles were basically the same. Oh DY *et al.* used fresh tumor tissues from 21 patients with cervical cancer to establish a PDTX model, among which 14 were successful. In addition, it was found that the histopathological features of tumors from the cervical cancer PDTX model were completely consistent with those of primary tumors, and the expression of HER-2 was also highly consistent [12]. The PDTX model has been widely used in the research and development of new antitumor drugs, and has been successfully applied

130112Tumor volume

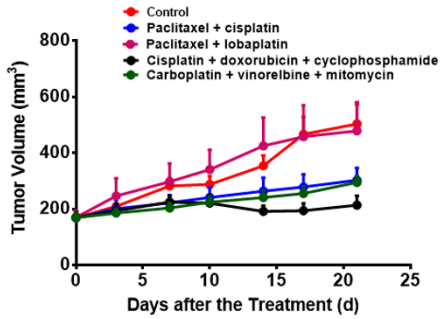

Mice weight

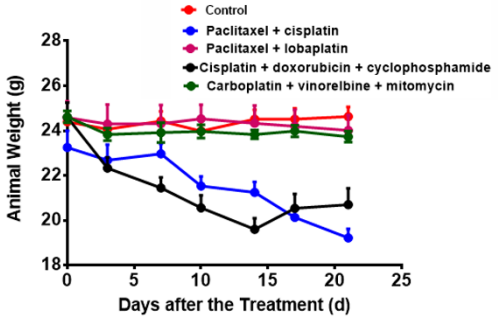

130140Tumor volume

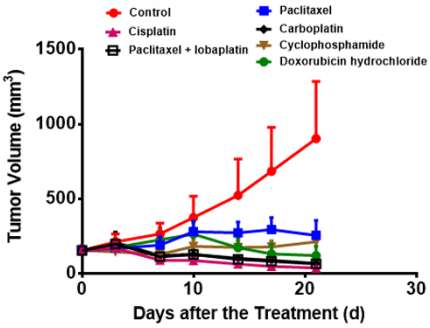

Mice weight

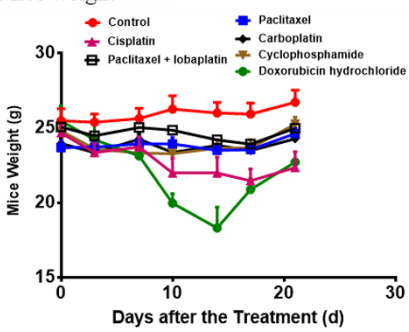

110158Tumor volume

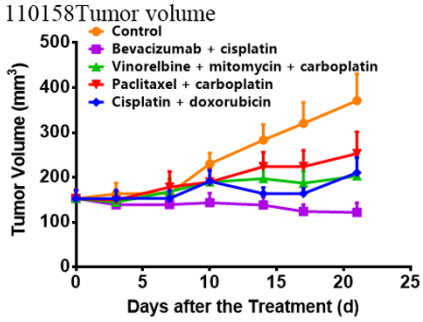

Mice weight

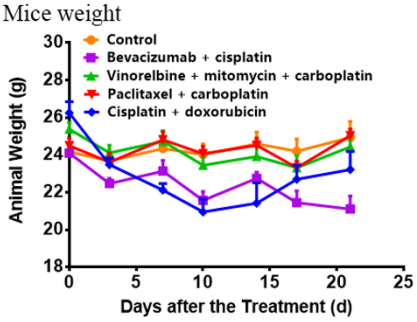

110164Tumor volume

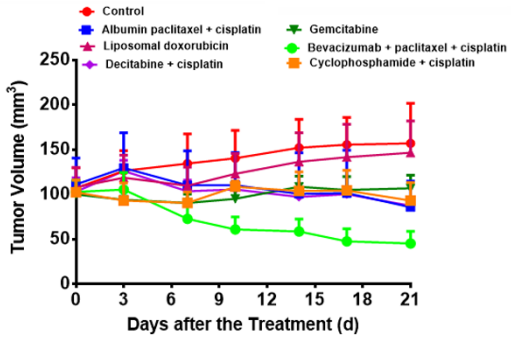

Mice weight

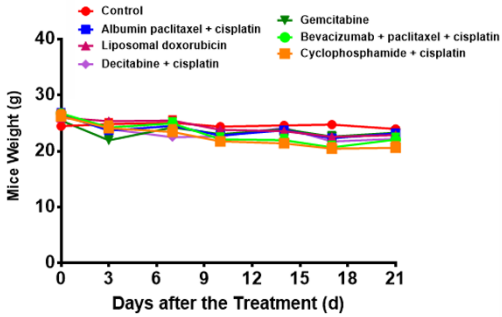

0101007Tumor volume

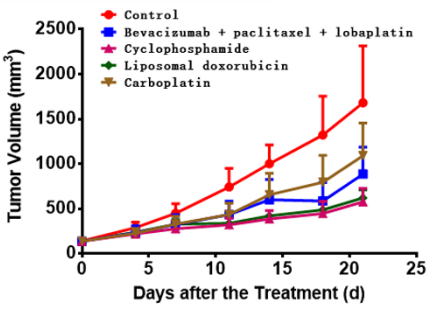

Mice weight

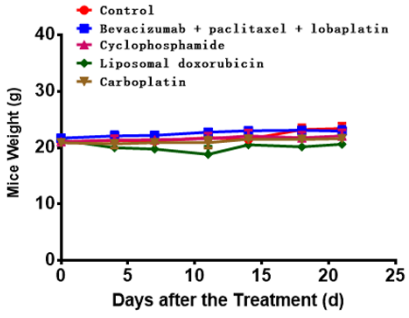

Figure 4. Pharmacodynamic curve: Pharmacodynamic tests were performed on five of the seven successful models, which involved 24 different therapeutic regimens. The therapeutic effect of each scheme varied in the PDTX models.

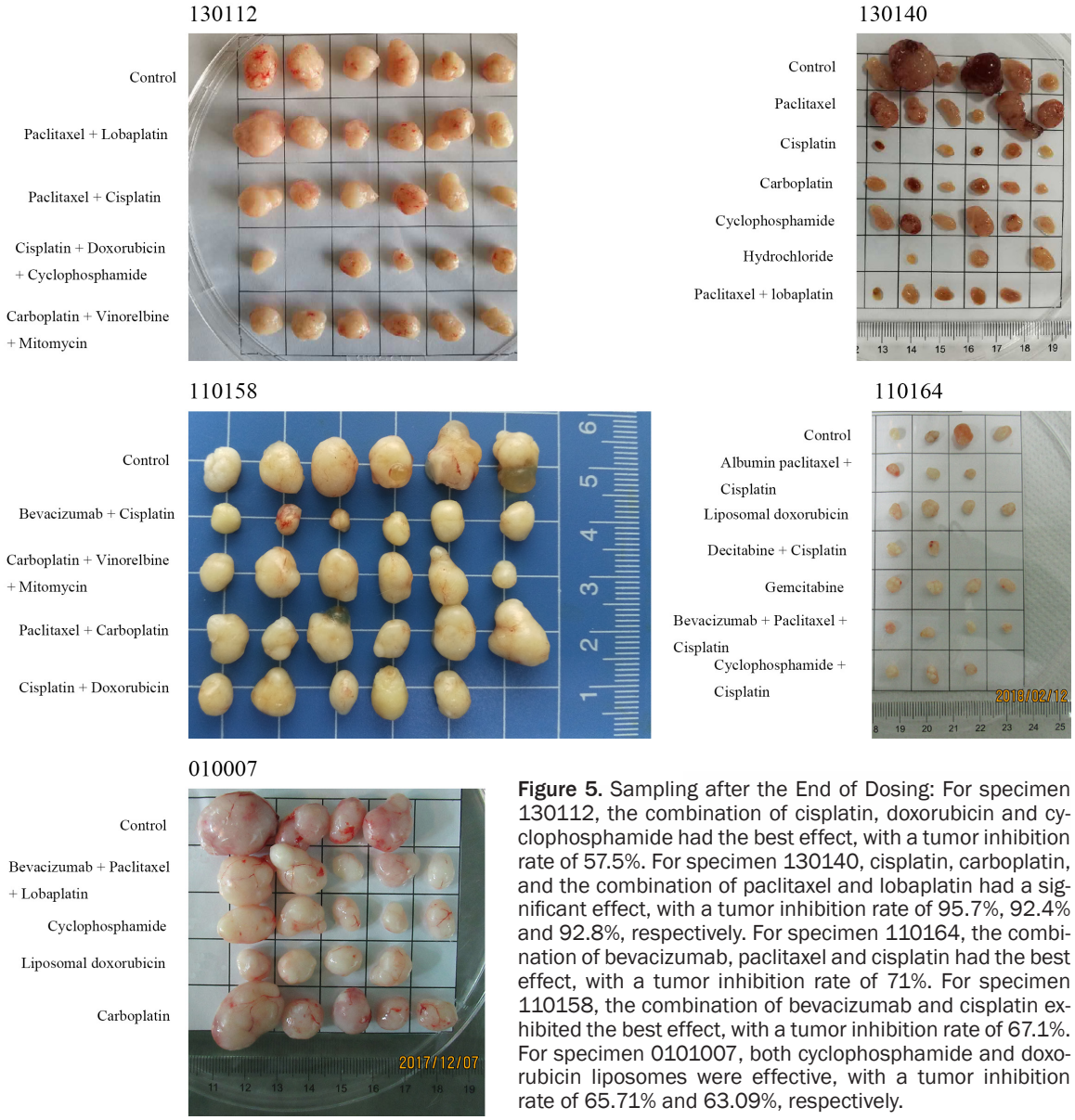

Figure 5. Sampling after the End of Dosing: For specimen 130112, the combination of cisplatin, doxorubicin and cyclophosphamide had the best effect, with a tumor inhibition rate of 57.5%. For specimen 130140, cisplatin, carboplatin, and the combination of paclitaxel and lobaplatin had a significant effect, with a tumor inhibition rate of 95.7%, 92.4% and 92.8%, respectively. For specimen 110164, the combination of bevacizumab, paclitaxel and cisplatin had the best effect, with a tumor inhibition rate of 71%. For specimen 110158, the combination of bevacizumab and cisplatin exhibited the best effect, with a tumor inhibition rate of 67.1%. For specimen 0101007, both cyclophosphamide and doxorubicin liposomes were effective, with a tumor inhibition rate of 65.71% and 63.09%, respectively.

in clinical practice in recent years. That is, the PDTX model has been used to test the pharmacodynamics of different therapeutic drugs and/or regimens *in vivo*, and the optimal therapeutic drugs and/or regimens can be selected as an important reference. Therefore, the clinical efficacy and safety of drug treatment can be significantly improved. Previous studies have revealed that the pharmacodynamic test based on the PDTX model could increase the efficiency of chemotherapy from 20%-30% to approximately 80%. Erriquez J *et al.* [13] established PDTX models using fresh ovarian cancer tissues obtained before and after neoadjuvant chemotherapy, and were treated with carboplatin, gemcitabine, liposomal doxorubicin and alkylating agent, respectively The results revealed that in the neoadjuvant chemotherapy-treated epithelial ovarian cancer model, the platinum-sensitive and platinum-resistant PDTX models had significant differences in platinum-like responses. In addition, the pharmacodynamic test results of the platinum-sensitive PDTX models revealed that carboplatin treat-

ment was effective, while platinum-based treatment in the platinum-resistant PDTX model was not effective, and this was consistent with clinical treatment results. The pharmacodynamic test results of the PDTX models in patients with platinum-resistance revealed that the effect of doxorubicin liposome was significant. In addition, the patient achieved complete response with the second-line treatment of doxorubicin liposome, which guided the clinical treatment. At the same time, these results indicated that the sensitivity of the patient model to the drug has also changed before and after neoadjuvant chemotherapy. In addition, trabectedin, an anti-soft tissue sarcoma drug, was more effective than carboplatin in the treatment of platinum-sensitive patients pretreated by neoadjuvant chemotherapy, thereby providing a broader choice for the treatment of these patients after recurrence. These results suggest that the PDTX model can be used to screen out the best individualized treatment regimen as an important clinical reference, in order to avoid the blind usage of medication, reduce side effects, and improve the quality of life and prolong the survival of patients.

In the present study, seven of 15 PDTX models were successful, with a success rate of 46.7%. The tumor formation time ranged from 21 days to 130 days, with a median formation time of 73 days. Pathological H&E staining was performed on tumor tissues obtained from five PDTX models, which were successfully modeled, and these were compared with the primary tumors obtained from patients. These results revealed that the pathological features of the PDTX models were consistent with those of primary tumors. Furthermore, this is consistent with the results of other researchers on different tumors, such as gastric cancer, liver cancer, lung cancer, colorectal cancer, melanoma and esophageal cancer, etc. Moreover, this also confirms that the PDTX model maintains the biological characteristics of primary tumors. Hence, it is a stable and reliable model for cancer research, thereby providing a good animal model for cancer research [14-16]. In the present study, five samples were screened for more effective drugs, and one of these was applied in clinic. For specimen 130112, the combination of cisplatin, doxorubicin and cyclophosphamide had the best effect, with a tumor inhibition rate of 57.5%. For specimen 130140, cisplatin, carboplatin, and the combination of paclitaxel and lobaplatin had a significant effect, with a tumor inhibition rate of 95.7%, 92.4% and 92.8%, respectively. For specimen 110158, the combination of bevacizumab and cisplatin exhibited the best effect, with a tumor inhibition rate of 67.1%. For specimen 0101007, both cyclophosphamide and doxorubicin liposomes were effective, with a tumor inhibition rate of 65.71% and 63.09%, respectively. The patient was initially treated with paclitaxel plus lobaplatin, and complete response was achieved during the chemotherapy. However, pleural, ascites and pelvic masses reappeared at two months after the cessation of chemotherapy, and tumor recurrence was confirmed by cytology. Based on the PDTX results, the chemotherapy regimen was changed to the combination of cyclophosphamide, doxorubicin liposome and cisplatin. At present, chemotherapy has been carried out for two courses, and the tumor markers significantly decreased, while the tumors shrunk.

The main factors that affected the success rate of the modeling included the following: (1) Tumor type and malignancy: This includes tumor classification, stage, differentiation, and malignancy. The higher the degree of malignancy, the higher the success rate of the modeling. (2) The degree of immunodeficiency in transplant recipients: At present, immunodeficient mice have been commonly used in the market, which mainly include nude mice, SCID, NOD/SCID, and NCG/NOG/NSG. The success rate of the modeling in NCG/NOG/NSG mice with a higher degree of immunodeficiency was relatively higher. (3) Tissue transport and transplantation procedures: The shorter the span between specimen collection and transplantation, the better the tissue viability, and the higher the success rate of the modeling. Pre-transplantation treatment, such as rinsing and removing impurities, including the surrounding blood and fat, selecting tissues with better viability, and performing transplantation at the position with a rich blood supply, can improve the modeling success rate, and facilitate the observation and measurement. (4) Recent chemotherapy history: For naïve patients, it is important to determine whether these patients received preoperative neoadjuvant chemotherapy before the sampling. According to the report of Dodbiba L *et al.* [17], when a patient received neoadjuvant chemotherapy before sampling, the modeling success rate was only

22%, while when the patient did not receive neoadjuvant chemotherapy before sampling, the modeling success rate was 78%. For relapsed patients, the longer the interval between the last chemotherapy and sampling time, the higher the success rate of the modeling. However, models with the histology, IHC and expression analysis of relevant marker genes remains unknown, and should be further researched.

The PDTX model preserves the biological characteristics of the primary tumor tissue and its response to drugs [2, 18-21]. It can be used to test a variety of drugs and/or regimens *in vivo*, in order to provide prioritization, thereby reducing the blindness of clinical medication. For early diagnosed platinum-resistant epithelial ovarian cancer, the chemotherapy regimen should be changed according to the results of the PDTX model. Therefore, the PDTX model can more effectively guide the individualized treatment of gynecologic cancer patients, in order to obtain the best clinical outcome [22].

Disclosure of conflict of interest

None.

Address correspondence to: Dr. Yuan-Guang Meng, Department of Obstetrics and Gynecology, Chinese PLA General Hospital, 28 Fuxing Road, Haidian District, Beijing 100853, China. Tel: +86 010-66938144; Fax: +86 010-66938144; E-mail: mengyuanguang2006@163.com

References

[1] Stordal B, Timms K, Farrelly A, Gallagher D, Busschots S, Renaud M, Thery J, Williams D, Potter J, Tran T, Korpanty G, Cremona M, Carey M, Li J, Li Y, Aslan O, O'Leary JJ, Mills GB, Hennessy BT. BRCA1/2 mutation analysis in 41 ovarian celllines reveals only one functionally deleterious BRCA1 mutation. Mol Oncol 2013; 7: 567-579.

[2] Tentler JJ, Tan AC, Weekes CD, Jimeno A, Leong S, Pitts TM, Arcaroli JJ, Messersmith WA, Eckhardt SG. Patient-derived tumour xenografts as models for oncology drug development. Nat Rev Clin Oncol 2012; 9: 338-350.

[3] Kopetz S, Lemos R, Powis G. The promise of patient-derived xenografts: the best laid plans of mice and men. Clin Cancer Res 2012; 18: 5160-5162.

[4] Šale S, Orsulic S. Models of ovarian cancer metastasis: murine models. Drug Discov Today Dis Models 2006; 3: 149-154.

[5] Boone JD, Dobbin ZC, Straughn JM Jr, Buchsbaum DJ. Ovarian and cervical cancer patient derived xenografts: the past, present, and future. Gynecol Oncol 2015; 138: 486-491.

[6] Callari M, Batra AS, Batra RN, Sammut SJ, Greenwood W, Clifford H, Hercus C, Chin SF, Bruna A, Rueda OM, Caldas C. Computational approach to discriminate human and mouse sequences in patient-derived tumour xenografts. BMC Genomics 2018; 19: 19.

[7] Heo EJ, Cho YJ, Cho WC, Hong JE, Jeon HK, Oh DY, Choi YL, Song SY, Choi JJ, Bae DS, Lee YY, Choi CH, Kim TJ, Park WY, Kim BG, Lee JW. Patient-derived xenograft models of epithelial ovarian cancer for preclinical studies. Cancer Res Treat 2017; 49: 915-926.

[8] Liu JF, Palakurthi S, Zeng Q, Zhou S, Ivanova E, Huang W, Zervantonakis IK, Selfors LM, Shen Y, Pritchard CC, Zheng M, Adleff V, Papp E, Piao H, Novak M, Fotheringham S, Wulf GM, English J, Kirschmeier PT, Velculescu VE, Paweletz C, Mills GB, Livingston DM, Brugge JS, Matulonis UA, Drapkin R. Establishment of patient-derived tumor xenograft models of epithelial ovarian cancer for preclinical evaluation of novel therapeutics. Clin Cancer Res 2017; 23: 1263-1273.

[9] Eoh KJ, Chung YS, Lee SH, Park SA, Kim HJ, Yang W, Lee IO, Lee JY, Cho H, Chay DB, Kim S, Kim SW, Kim JH, Kim YT, Nam EJ. Comparison of clinical features and outcomes in epithelial ovarian cancer according to tumorigenicity in patient-derived xenograft models. Cancer Res Treat 2018; 50: 956-963.

[10] Ricci F, Fratelli M, Guffanti F, Porcu L, Spriano F, Dell'Anna T, Fruscio R, Damia G. Patient-derived ovarian cancer xenografts re-growing after a cisplatinum treatment are less responsive to a second drug re-challenge: a new experimental setting to study response to therapy. Oncotarget 2017; 8: 7441-7451.

[11] Colombo PE, du Manoir S, Orsett B, Bras-Gonçalves R, Lambros MB, MacKay A, Nguyen TT, Boissière F, Pourquier D, Bibeau F, Reis-Filho JS, Theillet C. Ovarian carcinoma patient derived xenografts reproduce their tumor of origin and preserve an oligoclonal structure. Oncotarget 2015; 6: 28327-28340.

[12] Oh DY, Kim S, Choi YL, Cho YJ, Oh E, Choi JJ, Jung K, Song JY, Ahn SE, Kim BG, Bae DS, Park WY, Lee JW, Song S. HER2 as a novel therapeutic target for cervical cancer. Oncotarget 2015; 6: 36219-36230.

[13] Erriquez J, Olivero M, Mittica G, Scalzo MS, Vaira M, De Simone M, Ponzone R, Katsaros D, Aglietta M, Calogero R, Di Renzo MF, Valabrega G. Xenopatients show the need for precision medicine approach to chemotherapy in ovarian cancer. Oncotarget 2016; 7: 26181-26191.

[14] Hao C, Wang L, Peng S, Cao M, Li H, Hu J, Huang X, Liu W, Zhang H, Wu S, Pataer A, Heymach JV, Eterovic AK, Zhang Q, Shaw KR, Chen K, Futreal A, Wang M, Hofstetter W, Mehran R, Rice D, Roth JA, Sepesi B, Swisher SG, Vaporciyan A, Walsh GL, Johnson FM, Fang B. Gene mutations in primary tumors and corresponding patient-derived xenografts derived from non-small cell lung cancer. Cancer Lett 2015; 357: 179-185.

[15] Zhu Y, Tian T, Li Z, Tang Z, Wang L, Wu J, Li Y, Dong B, Li Y, Li N, Zou J, Gao J, Shen L. Establishment and characterization of patient-derived tumor xenograft using gastroscopic biopsies in gastric cancer. Sci Rep 2015; 5: 8542.

[16] Gu Q, Zhang B, Sun H, Xu Q, Tan Y, Wang G, Luo Q, Xu W, Yang S, Li J, Fu J, Chen L, Yuan S, Liang G, Ji Q, Chen SH, Chan CC, Zhou W, Xu X, Wang H, Fang DD. Genomic characterization of a large panel of patient-derived hepatocellular carcinoma xenograft tumor models for preclinical development. Oncotarget 2015; 6: 20160-20176.

[17] Dodbiba L, Teichman J, Fleet A, Thai H, Sun B, Panchal D, Patel D, Tse A, Chen Z, Faluyi OO, Renouf DJ, Girgis H, Bandarchi B, Schwock J, Xu W, Bristow RG, Tsao MS, Darling GE, Ailles LE, El-Zimaity H, Liu G. Primary esophageal and gastro-esophageal junction cancer xenograft models: clinicopathological features and engraftment. Lab Invest 2013; 93: 397-407.

[18] Julien S, Merino-Trigo A, Lacroix L, Pocard M, Goéré D, Mariani P, Landron S, Bigot L, Nemati F, Dartigues P, Weiswald LB, Lantuas D, Morgand L, Pham E, Gonin P, Dangles-Marie V, Job B, Dessen P, Bruno A, Pierré A, De Thé H, Soliman H, Nunes M, Lardier G, Calvet L, Demers B, Prévost G, Vrignaud P, Roman-Roman S, Duchamp O, Berthet C. Characterization of a large panel of patient-derived tumor xenografts representing the clinical heterogeneity of human colorectal cancer. Clin Cancer Res 2012; 18: 5314-5328.

[19] Scott CL, Becker MA, Haluska P, Samimi G. Patient-derived xenograft models to improve targeted therapy in epithelial ovarian cancer treatment. Front Oncol 2013; 3: 295.

[20] Siolas D, Hannon GJ. Patient-derived tumor xenografts: transforming clinical samples into mouse models. Cancer Res 2013; 73: 5315-5319.

[21] Rosfjord E, Lucas J, Li G, Gerber HP. Advances in patient-derived tumor xenografts: from target identification to predicting clinical response rates in oncology. Biochem Pharmacol 2014; 91: 135-143.

[22] Malaney P, Nicosia SV, Davé V. One mouse, one patient paradigm: new avatars of personalized cancer therapy. Cancer Lett 2014; 344: 1-12.